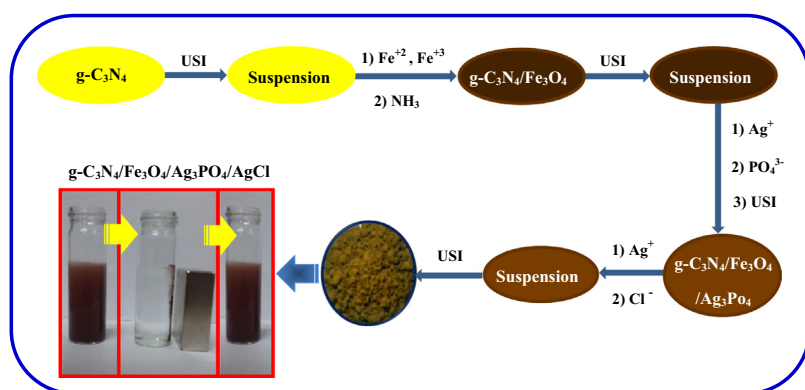Regular Article

Fabrication of novel magnetically separable nanocomposites using graphitic carbon nitride, silver phosphate and silver chloride and their applications in photocatalytic removal of different pollutants using visible-light irradiation

Mitra Mousavi [a], Aziz Habibi-Yangjeh [a,*], Masoud Abitorabi [b]

[a] Department of Chemistry, Faculty of Science, University of Mohaghegh Ardabili, P.O. Box 179, Ardabil, Iran
[b] Department of Civil Engineering, University of Mohaghegh Ardabili, P.O. Box 179, Ardabil, Iran

GRAPHICAL ABSTRACT

ABSTRACT

In the present study, g-C$_3$N$_4$/Fe$_3$O$_4$/Ag$_3$PO$_4$/AgCl nanocomposites endowed with efficient photocatalytic activity under visible-light irradiation have been successfully prepared by a facile ultrasonic-irradiation method. The prepared samples were characterized by XRD, EDX, AAS, SEM, TEM, UV–vis DRS, FT-IR, TG, PL, and VSM techniques. Rhodamine B, methyl orange, fuchsine, and phenol were selected as pollutants to evaluate photocatalytic activity of the as-prepared samples. Among the samples, the g-C$_3$N$_4$/Fe$_3$O$_4$/Ag$_3$PO$_4$/AgCl (30%) nanocomposite displayed the highest photocatalytic activity. It was found that activity of this nanocomposite in degradation of rhodamine B is nearly 22, 6, and 7.5-times higher than those of the g-C$_3$N$_4$, g-C$_3$N$_4$/Fe$_3$O$_4$/Ag$_3$PO$_4$ (20%), and g-C$_3$N$_4$/Fe$_3$O$_4$/AgCl (30%) samples, respectively. The significant amount of saturation magnetization (8.78 emu g^{-1}) for this nanocomposite indicated that the photocatalyst can be easily separated from the treated solution using a magnetic field. According to the trapping experiments, it was found that holes are main active species, driving the degradation reaction. This work suggests that the quaternary nanocomposite is promising photocatalyst for degradation of organic pollutants under visible-light illumination.

© 2016 Elsevier Inc. All rights reserved.

* Corresponding author.
    E-mail address: ahabibi@uma.ac.ir (A. Habibi-Yangjeh).

1. Introduction

In recent decades, synthetic dyes are widely used in different industries such as textile, leather, paper, and food. With huge development of these industries, due to large-scale production and extensive applications of these dyes, they cause major environmental pollution in aquatic systems [1]. Hence, removal of such toxic compounds from the environment is a major issue for researchers. Among different methods for removing these pollutants, heterogeneous photocatalysis has emerged as the most promising green technology [2,3]. It is noteworthy to say that this green technology is used in different disciplines including inactivation of microorganisms, production of hydrogen gas, reduction of carbon dioxide to small molecules of fuels, and synthesis of various organic compounds [2–6]. However, in order to use effectively the solar energy in photocatalytic processes, it is necessary to provide a photocatalyst with band gap less than about 2.7 eV; hence, designing visible-light-driven photocatalysts with considerable activity is an active research field [7,8].

In the searching for effective visible-light-driven photocatalysts, graphitic carbon nitride (g-C_3N_4) has recently attracted tremendous attention [9]. The heptazine ring structure and the high condensation degree enable this metal-free semiconductor to possess many advantages such as good physicochemical properties, as well as appealing electronic structure with a medium band gap [10,11]. Unique properties of high stability (even in strong acidic and alkaline solutions), low cost, and band gap of 2.7 eV make g-C_3N_4 a promising candidate for photocatalytic processes utilizing the solar energy as light source [9–12]. Nevertheless, pure g-C_3N_4 suffers from rapid recombination of photogenerated charge carriers and poor absorption in visible region, resulting in low photocatalytic activity under visible-light illumination [11,12]. As a result, the exploration of g-C_3N_4-based photocatalysts with enhanced photocatalytic activities is of increasing importance [10–15]. In recent years, some strategies such as doping of metallic or nonmetallic elements, enhancing surface area, and coupling with other semiconductors have been employed to enhance photocatalytic activity of g-C_3N_4 [12]. Silver phosphate (Ag$_3$PO$_4$) has been proven to be a promising visible-light-driven photocatalyst, due to narrow band gap of 2.45 eV and quantum efficiency of nearly 90% [16]. Hence, some authors have prepared g-C_3N_4/Ag$_3$PO$_4$ photocatalysts and their enhanced photocatalytic activities relative to the pure g-C_3N_4 have been investigated under visible-light irradiation [17–23].

It is well known that separation of photocatalysts from treated solutions is another challenge for commercialization of photocatalytic processes [24]. It was found that combining magnetic materials by photocatalysts is an effective way to separate photocatalysts from the photocatalytic systems using an external magnetic field [24–29]. Among different magnetic materials, Fe$_3$O$_4$ nanoparticles have attracted much interests, because of their considerable saturation magnetizations [30]. Literature review exhibited that not only there is not any research about magnetically separable photocatalysts containing g-C_3N_4 and Ag$_3$PO$_4$, but also there is not any report about preparation and investigation photocatalytic activity of g-C_3N_4/Fe$_3$O$_4$/Ag$_3$PO$_4$/AgCl nanocomposites, as magnetically recoverable visible-light-driven photocatalysts.

In these regards, we prepared g-C_3N_4/Fe$_3$O$_4$/Ag$_3$PO$_4$/AgCl nanocomposites by a facile ultrasonic-irradiation method, for the first time. The photocatalytic performances were evaluated by photodegradation of rhodamine B (RhB) under visible-light irradiation. The effects of Ag$_3$PO$_4$ and AgCl contents on the photocatalytic activity were also investigated. In addition, the photodegradation mechanism over the g-C_3N_4/Fe$_3$O$_4$/Ag$_3$PO$_4$/AgCl was also discussed. The results revealed that weight percent of Ag$_3$PO$_4$ and AgCl, ultrasonic-irradiation time, calcination temperature, and scavengers of the reactive species have remarkable influence on the degradation reaction. Finally, ability of the nanocomposite for degradation of methyl orange (MO), fuchsine, and phenol was confirmed.

2. Experimental

2.1. Materials

Ferric chloride (FeCl$_3$·6H$_2$O, 99.5%), ferrous chloride (FeCl$_2$·4H$_2$O, 98.0%), ammonia solution (30%), melamine (C$_3$H$_6$N$_6$, 99.2%), silver nitrate (99.9%), sodium hydroxide (98%), sodium chloride (99.5%), and benzoquinone were purchased from Loba Chemie and used without further purifications. Sodium phosphate (Na$_2$HPO$_4$·2H$_2$O, 97%) was purchased from Rankem. Hydrochloric acid (HCl), 2-propanol, ammonium oxalate, RhB, MO, fuchsine, phenol, and absolute ethanol with high quality were obtained from Merck. Deionized water was used throughout this work.

2.2. Instruments

The X-ray diffraction (XRD) patterns were recorded by a Philips Xpert X-ray diffractometer with Cu Kα radiation (λ = 0.15406 nm), employing scanning rate of 0.04°/s in the 2θ range from 20° to 80°. Surface morphology and distribution of particles were studied by LEO 1430VP scanning electron microscopy (SEM), using an accelerating voltage of 15 kV. The purity and elemental analysis of the products were obtained by energy dispersive analysis of X-rays (EDX) on the same SEM instrument. For SEM and EDX experiments, samples were mounted on an aluminum support using a double adhesive tape coated with a thin layer of gold. The transmission electron microscopy (TEM) investigations were performed by a Zeiss-EM10C instrument with an acceleration voltage of 80 kV. The UV–vis diffuse reflectance spectra (DRS) were recorded by a Scinco 4100 apparatus. The Fourier transform-infrared (FT-IR) spectra were obtained by a Perkin Elmer Spectrum RX I apparatus. The photoluminescence (PL) spectra of the samples were studied using a Perkin Elmer (LS 55) fluorescence spectrophotometer with an excitation wavelength of 300 nm. The conditions were fixed in order to compare the PL intensities. The UV–vis spectra during the degradation reactions were studied using a Cecile 9000 spectrophotometer. Magnetic properties of the samples were obtained using an alternating gradient force magnetometer (model AGFM, Iran). The contents of Fe and Ag in the g-C_3N_4/Fe$_3$O$_4$/Ag$_3$PO$_4$/AgCl (30%) nanocomposite was determined by atomic absorption spectroscopy (AAS) by Analytik Jena of model ContrAA 700. The pH of solutions was measured using a Metrohm digital pH meter of model 691. The ultrasound radiation was performed using a Bandeline ultrasound processor HD 3100 (12 mm diameter Ti horn, 75 W, 20 kHz).

2.3. Preparation of the photocatalysts

The g-C_3N_4 powder was prepared by heating melamine powder up to 520 °C [9]. The required water in this section was degassed by bubbling N$_2$ gas for 20 min. The g-C_3N_4/Fe$_3$O$_4$ (2:1) nanocomposite, where 2:1 is weight ratio of g-C_3N_4 to Fe$_3$O$_4$, was prepared according to our previous work [29]. The g-C_3N_4/Fe$_3$O$_4$/Ag$_3$PO$_4$ (20%) nanocomposite was prepared by ultrasonic-irradiation method. In a typical method, 0.4 g of the g-C_3N_4/Fe$_3$O$_4$ (2:1) nanocomposite was dispersed into 150 mL of water by ultrasonic irradiation for 5 min. Then, 0.122 g of silver nitrate was added to the suspension and stirred for 60 min at room